Creation and purification of photonic entanglement from self-assembled quantum dots

A thesis presented for the degree of
Master of Science

Master's Degree Program in Photonics and Nanoelectronics
Department of Physics
University of Crete
February 2021

Master's Thesis

Creation and purification of photonic entanglement from self-assembled quantum dots

Μεταπτυχιακή Διπλωματική Εργασία

Δημιουργία και κάθαρση φωτονικής σύμπλεξης από αυτοσυναρμολογούμενες κβαντικές τελείες

Rafail Frantzeskakis

Thesis supervisor: Prof. Sophia Economou, Virginia Tech
Examination committee:
Prof. Alexandros Georgakilas (Advisor at Univ. Crete)
Prof. Eleftherios Economou
Prof. Ioannis Kominis

Master's Degree Program in Photonics and Nanoelectronics
Department of Physics
University of Crete
March 2021

Abstract

"Cluster" and "graph" states are entangled quantum states that are crucial resources in measurement-based quantum computing and quantum communications. Despite the importance of photonic graph and cluster states for quantum technologies, their generation presents considerable difficulties and it is a matter of current research.

Semiconductor quantum dots (QDs) are strong candidates for creating photonic cluster and graph states. In the first part of the thesis, we will study the generation and characterization of entangled photonic states from self-assembled quantum dots. Then we will investigate the purification of these states to maximize the overlap with the target entangled state.

Acknowledgments

First and foremost, I am very grateful to my master thesis advisor Sophia Economou for her continuous help, patience, and her guidance throughout the whole thesis. I am very thankful for giving me the opportunity of studying quantum physics and learning more about the subject through fruitful discussions.

Also I want to thank my family and my friends that supported me constantly throughout this journey.

Contents

1 Quantum Information Processing

Quantum Information Processing is a field that studies the transmission and manipulation of information taking advantage of quantum mechanics. Quantum information science is applied to different branches of science. In the following sections, we will analyze the basics of quantum information science.

1.1 Qubit

The first and most fundamental concept of quantum information is the qubit. Generally speaking, a qubit is a two-level system. Qubits are electrons in quantum dots or photons.

Di Vincenzo proposed the necessities for a two-level system to be prepared in a quantum computer as a qubit.[1] In this thesis, we will focus on the initialization and manipulation of qubits in a quantum dot.

1.2 Bloch Sphere

The geometrical representation of a two-level system is the Bloch sphere. The state $|\Psi\rangle$ of the two-level system is a Bloch vector that points in the surface of the unit sphere.

$$|\Psi\rangle = \cos\frac{\theta}{2}|0\rangle + e^{i\phi}\sin\frac{\theta}{2}|1\rangle \tag{1.2.1}$$

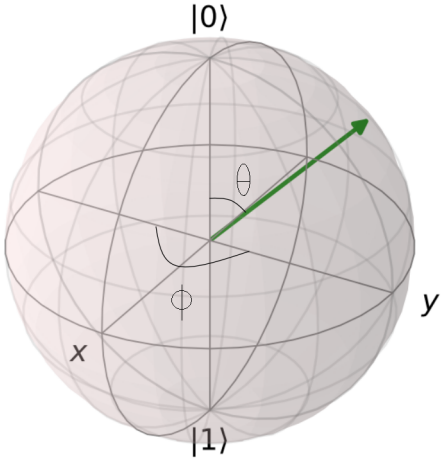

Figure 1: Every qubit state can be represented on Bloch sphere.

1.2.1 Rotations in Bloch sphere

Any vector on the Bloch sphere represents a quantum state. To manipulate the qubit we have to make rotations around an arbitrary axis. These rotations are essential for the initialization of qubits. The rotations will change the phase and amplitudes of the ground and excited state of the two-level system. Rotations can be performed about an arbitrary axis. The three fundamental rotations are about the x, y and z-axis.

$$R_x(\phi) = e^{-iX\frac{\phi}{2}} = \cos\frac{\phi}{2}I - i\sin\frac{\phi}{2}X = \begin{pmatrix} \cos\frac{\phi}{2} & -i\sin\frac{\phi}{2} \\ -i\sin\frac{\phi}{2} & \cos\frac{\phi}{2} \end{pmatrix}$$

$$R_y(\phi) = e^{-iY\frac{\phi}{2}} = \cos\frac{\phi}{2}I - i\sin\frac{\phi}{2}Y = \begin{pmatrix} \cos\frac{\phi}{2} & \sin\frac{\phi}{2} \\ -\sin\frac{\phi}{2} & \cos\frac{\phi}{2} \end{pmatrix}$$

$$R_z(\phi) = e^{-iZ\frac{\phi}{2}} = \cos\frac{\phi}{2}I - i\sin\frac{\phi}{2}Z = \begin{pmatrix} e^{-i\frac{\phi}{2}} & 0 \\ 0 & e^{i\frac{\phi}{2}} \end{pmatrix}$$

To rotate our state by any arbitrary angle we will need a linear combination of the three fundamental rotations. We can initialize our qubit in every state we want through rotations. After the successful initialization, the qubit is prepared for any quantum computation.

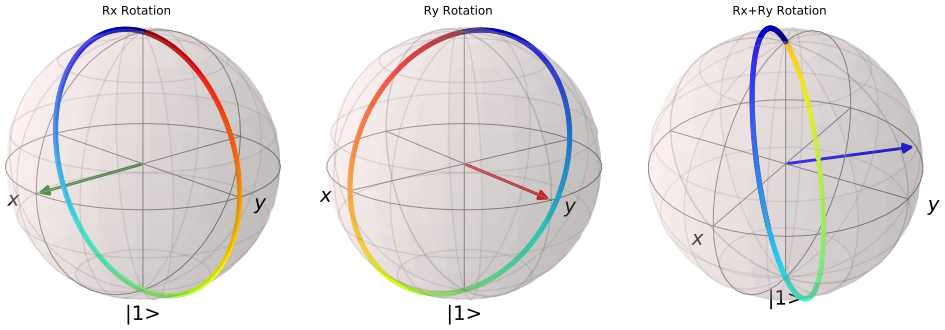

(a) Rx rotation (b) Ry rotation (c) Rx+Ry rotation

The optical rotations of a qubit by a specific axis can be done with coherent pulses in the qubit space directly or indirectly. In the direct process, the pulse is applied in the desired two-level system and the transfer of population is affected by the pulse width and detuning. There is another way of rotating the qubit by using the excited state in the Λ system.[3, 4]

1.3 Two-qubit Entanglement

Apart from initialization and manipulation of qubits, the most quantum mechanical property of matter is the entanglement, the quantum correlation between qubits, which has no classical analog.

1.3.1 Definition

Suppose that we have two qubits that define a Hilbert space of 2^2 dimensions. In the bipartite system, the whole state Ψ of the two **entangled** qubits in general **cannot** be written in the following way.

$$\Psi = \psi_0 \otimes \psi_1 \tag{1.3.1}$$

When the state can be written as (1.3.1) it is separable. Every qubit acts in its own Hilbert space with no correlation with the other one. If we use **L**ocal **O**perations and **C**lassical **C**ommunication (LOOC) there is no way to make the state (1.3.1) an entangled state.

1.3.2 Entangling gates

To entangle two qubits there is a way of applying entangling gates in the tensor product of the two systems. Two of the most well-known entangling gates are CNOT and Cphase gate.

$$\text{CNOT} = \begin{pmatrix} 1 & 0 & 0 & 0 \\ 0 & 1 & 0 & 0 \\ 0 & 0 & 0 & 1 \\ 0 & 0 & 1 & 0 \end{pmatrix} \tag{1.3.2}$$

$$\text{Cphase} = \begin{pmatrix} 1 & 0 & 0 & 0 \\ 0 & 1 & 0 & 0 \\ 0 & 0 & 1 & 0 \\ 0 & 0 & 0 & e^{i\theta} \end{pmatrix} \tag{1.3.3}$$

There is a specific case of Cphase gate for angle $\theta = \pi$, the CZ gate.

We can use single-qubit gates and entangling ones to construct the four high entangled two-qubit states which are defined as Bell states[2]

$$\left|\Phi^{+,-}\right\rangle = \frac{|00\rangle \pm |11\rangle}{\sqrt{2}}$$
$$\left|\Psi^{+,-}\right\rangle = \frac{|01\rangle \pm |10\rangle}{\sqrt{2}}$$

The $|\Phi^{+}\rangle$ state is the well known GHZ state for two qubits. The GHZ state can be expanded in a multipartite entangled state as

$$|GHZ\rangle = \frac{|0\rangle^{\otimes N} + |1\rangle^{\otimes N}}{\sqrt{2}} \tag{1.3.4}$$

where N is the number of the qubits.

1.3.3 Experimental Entanglement

A famous example of creating photonic entanglement is Spontaneous Parametric Down Conversion(SPDC). The process is described below:

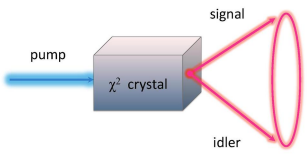

Figure 3: Spontaneous Parametric Down Conversion [5]

A strong laser of energy ω_i and wavenumber k_i pumps a nonlinear crystal. There is a small probability (1 success per $10^6 - 10^9$ incoming photons) of creating two entangled photons. The creation of entanglement depends on the interaction of the laser with the crystal. The process conserves the energy and the momentum. From a photon of energy ω_i we get two photons of generally different energies ω_1, ω_2 respectively where $\omega_i = \omega_1 + \omega_2$. The momentum is also conserved with the equation $k_i = k_1 + k_2$.

1.3.4 Entanglement Measures

The entanglement is not so trivial to be measured. In a theoretical approach, a simple way to measure the entanglement is by calculating the fidelity. Fidelity is a measure of how close is a state ψ to a target state ϕ.

$$F = |\langle\psi|\phi\rangle|^2$$

One other way for measuring the two-qubit entanglement is by looking at the concurrence. Concurrence is a quantity that varies from 0 to 1 for a highly entangled state. The calculation of concurrence in a pure entangled state $|\Psi\rangle$ is straightforward:

$$C = 2|c_{00}c_{11} - c_{01}c_{10}| \tag{1.3.5}$$

where c_{ij} are the coefficients of the general two qubit state $|\Psi\rangle = c_{00}|00\rangle + c_{01}|01\rangle + c_{10}|10\rangle + c_{11}|11\rangle$.

Another way to measure entanglement is by quantum state tomography. Quantum state tomography (QST) is a process that results in the full construction of the density matrix of the desired state.[2] It is a direct reconstruction of a density matrix that can detect any quantum correlations if there are nondiagonal density matrix elements.

Moreover, the stabilizer operators S are useful for the measure of entanglement. A stabilizer operator is a tensor product of Pauli operators that stabilizes the desired state. In other words, stabilizers satisfy the eigenvalue equation with eigenvalue + 1.

$$S|\psi\rangle = +|\psi\rangle$$

For the whole system of 2^n stabilizer operators, the entanglement measure is the mean value of all stabilizer operators and varies from zero to one. If the mean value is one then the state is highly entangled.[2]

1.4 Multipartite Entanglement

Going beyond the entanglement between two systems we define multipartite entanglement. Multipartite entanglement is much more complicated. There is no full understanding of high-dimensional entangled states.

Instead of having two systems, we can define the entanglement between N systems. Multipartite entangled states, in general, **cannot** be written as:

$$\Psi = \psi_o \otimes .... \otimes \psi_i \otimes ..... \otimes \psi_N \tag{1.4.1}$$

Quantifying entanglement in higher entangled states is not trivial. A way of identifying multipartite entanglement is by looking at quantities such as entanglement witnesses or stabilizers.[6, 7]

1.4.1 Graph states

Graph states are multi-qubit entangled states that can be represented graphically. A graph state G is defined by its vertices (qubits) V and edges E that connect a vertex with another one. So, the edges represent the entanglement between the qubits. A more mathematical description of graph states is :

$$G(V,E) = \prod_{a,b \in E} CZ^{a,b} \left|+\right\rangle^{\otimes N} \tag{1.4.2}$$

where the vertices are represented in state $\left|+\right\rangle = \frac{\left|0\right\rangle + \left|1\right\rangle}{\sqrt{2}}$ and the entanglement is generated through the CZ gate.

Another way to define a graph state is the *adjacency matrix*. The adjacency matrix is a square matrix that represents a graph. This matrix is an NxN matrix for a graph state with N vertices. The elements of this matrix are defined as:

$$\Gamma_{a,b} = 1 \; if \; a,b \in E \quad otherwise \; \Gamma_{a,b} = 0 \tag{1.4.3}$$

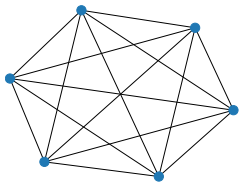

Figure 4: Star (complete) graph with adjacency matrix $\Gamma_{ij \; i \neq j} = 1$

2-colorable graphs
Each vertex represents a specific qubit of a physical system. In the following figure, the spin is the green vertex and the photon is red. The edges between them represent the entanglement between spin and photon.

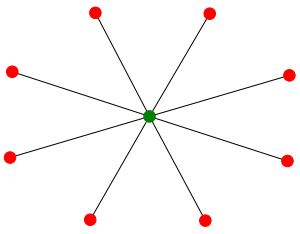

Figure 5: Graphical GHZ state with adjacency matrix $\Gamma_{1,j} = \Gamma_{j,1} = 1$

k-colorable graphs
In addition to 2-colorable graphs, k-colorable are even broader. A graph is called a k-colorable graph if it is possible to divide the vertices of each graph into a group and assign it to each group color such that no neighbor vertices have the same color. So, a *group of vertices* is defined as the number of vertices that are not connected through edges (next nearest neighbors). In the following examples, there are three groups of vertices (green, red, blue).[8, 9]

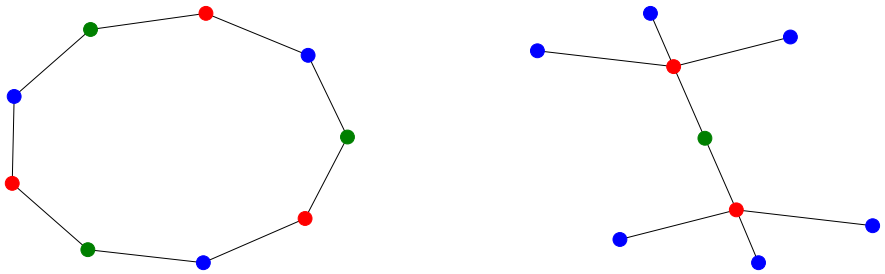

(a) Circle 3-colorable graph

(b) Tree 3-colorable graph

1.4.2 Cluster states

One category of graph states is cluster states that are highly entangled and are represented by vertices in $|+\rangle$ states with a CZ gate between them which are represented in 1D, 2D, and 3D square lattices.

$$G(V, E) = \prod_{a,b \in E} CZ^{a,b} |+\rangle^{\otimes N} \tag{1.4.4}$$

Real examples of cluster states can be made through cold atoms in optical lattices.[10] There is a possibility of making cluster states using sequential quantum dots taking advantage of tunneling, making coupled quantum dots. [11, 12]

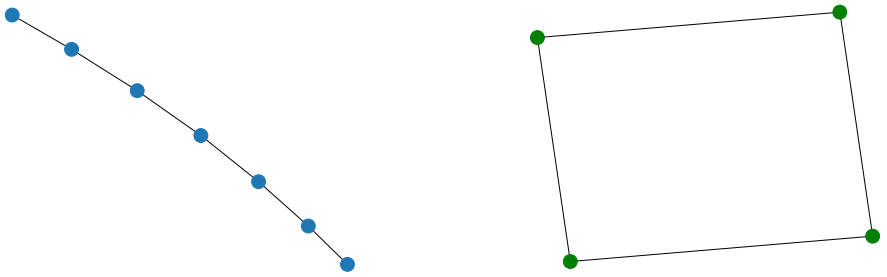

(a) 1d Cluster state (b) 2d Cluster state

1.4.3 Measurement Based Quantum Computing

The above graphs and especially cluster states are the resource states for measurement-based quantum computation.

Measurement-based quantum computing is a model of quantum computation that was introduced in 2001.[13] In this type of quantum computation, the resource state is a 2D cluster state.[12] After the initialization of this entangled state, we can apply only single-qubit operations and classical feed-forward measurements to perform quantum computations.

The advantage of this computation is that it does not require two-qubit gates during the computation. These gates are, in general, difficult to be performed. In this model, the difficulty of creating entanglement has been transferred to the preparation of the cluster state.

2 Self-assembled quantum dots

Quantum dots are promising systems for quantum technologies and generally in the study of quantum mechanics. Self-assembled semiconductor quantum dots are single-photon sources.[14] Their fast recombination rates are useful for the manipulation of qubits before interaction with the environment.[4]

2.1 Design of Self-assembled QDs

Self-assembled quantum dots are grown non-deterministically at the interface of two *different* semiconductor layers.

Specifically, a well-known example of self-assembled QDs are InAs and GaAs QDs. InAs QDs are formed using the Stranski-Krastanow growth.[4, 15] This growth mode utilizes the strain caused by the lattice mismatch between the InAs layers and GaAs substrates. On the other hand, GaAs self-assembled quantum dots are small islands that are formed due to the confinement with AlGaAs layers.[4]

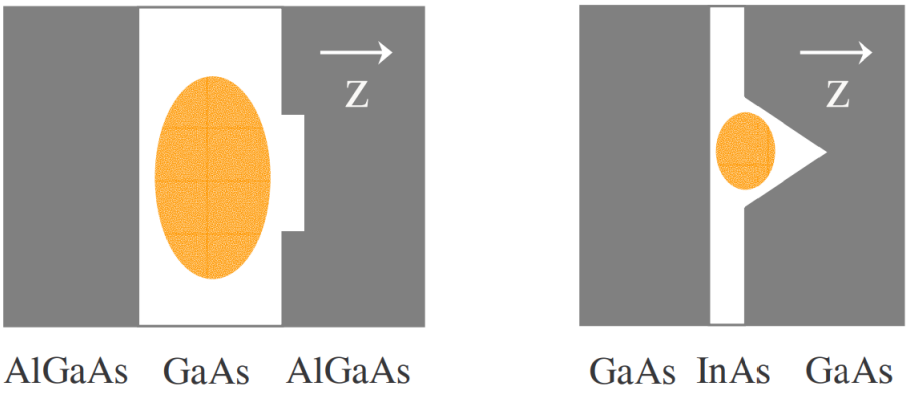

Figure 8: Formation of self-assembled QDs[4]

2.2 Structure

Experimentalists use semiconductors by taking advantage of their band structure to create single photons with specific polarization. The band structure of these materials consists of two bands the valence band and the conduction band. Each band has states that can be occupied by electrons. A direct or indirect energy bandgap is between valence and conduction band.

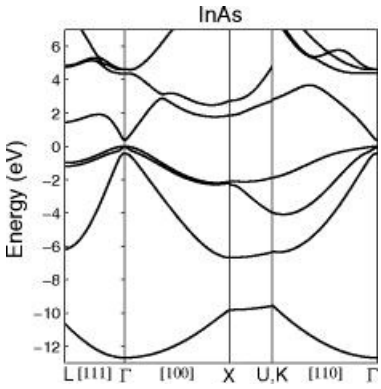

(a) InAs band structure[16]

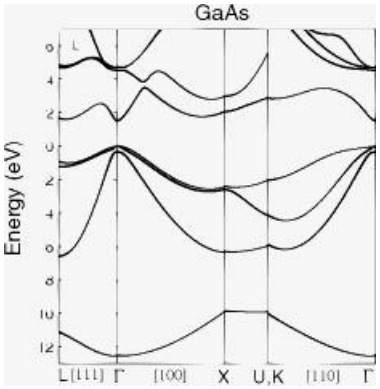

(b) GaAs band structure[16]

In absolute zero T=0 K, the valence band is fully occupied by electrons and the conduction band is empty. When an electron is excited optically, it jumps from the valence to the conduction band and leaves behind a hole in the valence band (absence of an electron). A pedagogical picture of seeing electrons and holes is exactly like bubbles in the water. The movement of water is the electron while bubbles are going to the top are the holes.

At low temperatures the electron-hole pair will depend on the spin configuration. So the exchange interaction of electrons with holes is responsible for the presence of excitons and their dynamics.

$$H_{ex} = a\vec{J_h} \cdot \vec{S_e} + b\vec{J_h^3} \cdot \vec{S_e} \tag{2.2.1}$$

where J_h is the hole's spin and S_e the electron's spin.[15]

2.2.1 Bulk and electronic states

The most popular semiconductor self-assembled quantum dots are designed between InAs and GaAs parts. InAs and GaAs are in the zincblende lattice structure. We can identify their band structure by looking at their lattice structure.

The valence band consists of electrons that are mainly formed in p-type orbitals. About the conduction band, the electrons are formed in s orbitals near the edge of this band. States of holes and electrons in valence (v) and conduction band (c)[11]:

$$|c\rangle_{1/2}^{1/2} = |s\rangle\,|\uparrow\rangle \text{ Electron spin up}$$
$$|c\rangle_{-1/2}^{1/2} = |s\rangle\,|\downarrow\rangle \text{ Electron Spin down}$$
$$|v\rangle_{3/2}^{3/2} = -\frac{1}{\sqrt{2}}\,|x+iy\rangle\,|\uparrow\rangle \text{ Heavy hole up}$$
$$|v\rangle_{-3/2}^{3/2} = \frac{1}{\sqrt{2}}\,|x-iy\rangle\,|\downarrow\rangle \text{ Heavy hole down}$$
$$|v\rangle_{1/2}^{3/2} = -\frac{1}{\sqrt{6}}(|x+iy\rangle\,|\downarrow\rangle + 2\,|z\rangle\,|\uparrow\rangle) \text{ Light hole}$$
$$|v\rangle_{-1/2}^{3/2} = \frac{1}{\sqrt{6}}(|x-iy\rangle\,|\uparrow\rangle + 2\,|z\rangle\,|\downarrow\rangle) \text{ Light hole}$$
$$|v\rangle_{1/2}^{1/2} = -\frac{1}{\sqrt{3}}(|x+iy\rangle\,|\downarrow\rangle + |z\rangle\,|\uparrow\rangle) \text{ SO hole}$$
$$|v\rangle_{-1/2}^{1/2} = \frac{1}{\sqrt{3}}(|x-iy\rangle\,|\uparrow\rangle - |z\rangle\,|\downarrow\rangle) \text{ SO hole}$$

2.2.2 Excitons in QDs

Apart from single electrons or holes, there is a possibility of forming a system in QD which is an exciton. Excitons are bound states of electrons and holes with bulk binding energies $E_{b,bulk}\approx$ 0.2-2 meV and QD binding energies $E_{b,QD}\approx$ 2-100 meV for QD due to stronger confinement.[17]

In the spin configuration, the exciton can be presented as a heavy hole with an electron with a total spin of $J = 1$.

2.2.3 Trions in QDs

Trions are charged excitons. There are two types of charged excitons, the negative one and the positive one. The positively charged exciton (t^+) consists of a single hole and an exciton (h-he). On the other hand, the negative trion is composed of an electron and an exciton. (t^-)

The trions are formed with an extra electron (t^-) or an extra hole (t^+) in the QD. The extra electron or hole is generated by a voltage difference. Current flows in the QD and it injects electrons in the desired state of the conduction band. Pauli's exclusion principle is blocking the continuous injection of electrons. The spin configuration of the electron -if it is in spin up

or down-state- can be seen by electrical current measurements.[18]

The trions are used for the excited state in the 3 level system. For example, a widely used three-level system in a simple self-assembled quantum dot consists of the following levels. The two ground states are the states of an extra electron in a conduction band under the application of a magnetic field.
The trion state forms the excited state of the Λ system.

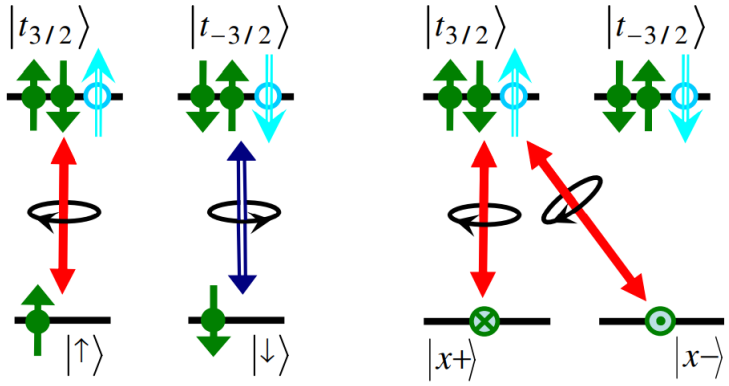

Figure 10: Trion and single electron states in QD[4]

where the green arrows are electrons and the cyan ones are holes.

2.2.4 Optical Transitions

The transitions help to manipulate the qubits in conduction and valence band. Selection rules for atomic systems are $\Delta J = 0, \pm 1$ and $\Delta m_j = \pm 1$ where j is the total angular momentum and m_j is the magnetic quantum number. The selection rules in the atomic or atomic-like systems (QDs) are conserved with the presence of light (photons).

The photon is a particle with helicity 1. Each photon carries a spin angular momentum. The possible spin angular momenta are $+\hbar$ and $-\hbar$ with a left circular polarization and right circular polarization respectively. Every linear combination of the polarization of photon can generate different transitions. The following table sums up the transition differences between matter and photons in QDs.

$$Mj_{electron} - Mj_{hole} = Mj_{photon}$$
$$J_{hole} - J_{electron} = 1$$

To satisfy the requirements for emitting a photon the conservation of total momentum and the magnetic quantum number is essential. In the following subsections, we will study the total transitions in which we are interested between electrons and trions in self-assembled QDs in different types of geometry.

2.2.5 Transitions in Faraday Geometry

A magnetic field in QDs is applied to split specific states on a different basis. We can work with a heavy hole or light hole trion system but in this case, we will investigate the heavy hole trion $|t\rangle^{3/2}_{\pm 3/2}$.

Faraday geometry is the application of a magnetic field parallel to the growth of the QD. This magnetic field is along the symmetry axis so the Zeeman energy splits the electron states but there is no splitting for trion states if there is a small magnetic field.

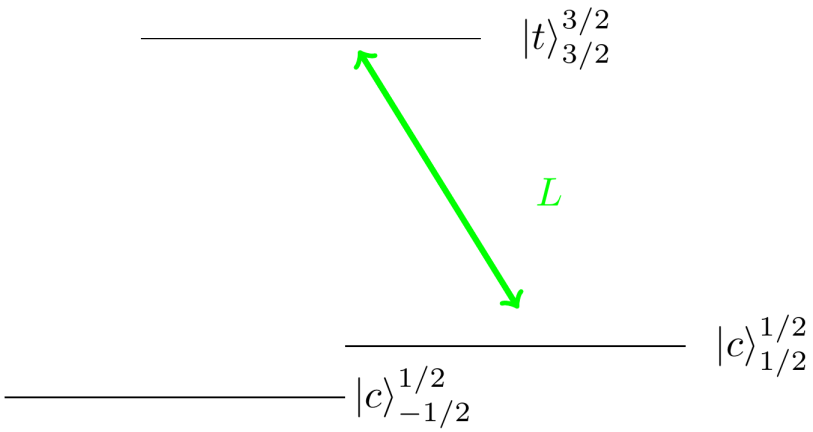

Figure 11: 3 level in Faraday Geometry

2.2.6 Transitions in Voigt Geometry

The Voigt geometry breaks the symmetry due to the application of a magnetic field along an axis perpendicular to the optical axis of the QD. This symmetry breaking changes the eigenstates of the system. The new eigenstates of the whole system are parallel to the direction of the field. For example, for a z-axis growth self-assembled quantum dot if the magnetic

field is on the x-axis the eigenstates of electron and heavy hole become:

$$|c\rangle^{1/2}_{1/2,x} = \frac{1}{\sqrt{2}}(|c\rangle^{1/2}_{1/2} + |c\rangle^{1/2}_{-1/2})$$
$$|c\rangle^{1/2}_{-1/2,x} = \frac{1}{\sqrt{2}}(|c\rangle^{1/2}_{1/2} - |c\rangle^{1/2}_{-1/2})$$
$$|v\rangle^{3/2}_{3/2,x} = \frac{1}{\sqrt{2}}(|v\rangle^{3/2}_{3/2} + |v\rangle^{3/2}_{-3/2})$$
$$|v\rangle^{3/2}_{-3/2,x} = \frac{1}{\sqrt{2}}(|v\rangle^{3/2}_{3/2} - |v\rangle^{3/2}_{-3/2})$$

So, there is a mixing of eigenstates on a z basis if we apply an x-axis magnetic field. The x-axis magnetic field is willing to make possible indirect transitions.

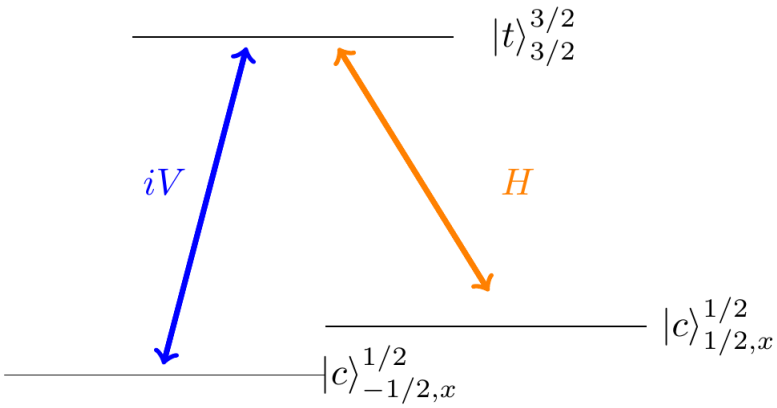

Figure 12: 3 level in Voigt Geometry

2.3 QDs with semiclassical field

We will present the main types of level systems that are used in semiconductor self-assembled quantum dots in the presence of laser.

2.3.1 Two-level system

The simplest example of a two-level system in QD is an electron under the application of a magnetic field. There is a split in energies which makes the lower energy represent the $|0\rangle$ state, and the higher the $|1\rangle$ state. In a QD, there is another possibility of a two-level system with the ground state is the electron state and the excited state is the trion state. In this case, the dynamics of the system are governed by a pulsed or continuous laser with specific polarization.

2.3.2 Dynamics of two-level system

In this section, we will study how a two-level system in a QD behaves in the presence of a pulsed laser. We will investigate the spin vector dynamics in the Bloch sphere. For the dynamics of the system, we will solve the time-dependent Schrödinger equation in the presence of a pulse.
For the dynamics of the system, we solve the Schrödinger equation.

$$i\hbar\frac{\partial\Psi}{\partial t} = H\Psi \tag{2.3.1}$$

where $\Psi = c_g\,|g\rangle + c_e\,|e\rangle$.

The $|g\rangle, |e\rangle$ is the Dirac representation of the ground and excited-state respectively. The coefficients c_g, c_e are the amplitudes of the system. To be able to solve the problem we have to construct the Hamiltonian using the Rotating wave approximation (RWA).

$$H = -\frac{\hbar\omega_o}{2}\sigma_z + f(t)e^{i\omega t}\sigma_+ + f(t)e^{-i\omega t}\sigma_- \tag{2.3.2}$$

where $\sigma_+ = |e\rangle\langle g|, \sigma_- = |g\rangle\langle e|$. The $f(t)$ is the envelope function of the pulse .
We transform our Hamiltonian by going to the rotating frame.

$$U = \begin{pmatrix} e^{-i\omega_o t/2} & 0 \\ 0 & e^{i\omega_o t/2} \end{pmatrix} \tag{2.3.3}$$

Procced in interaction picture: V_I=$U^\dagger VU$ where $V = f(t)\sigma_- e^{-i\omega t} + f(t)\sigma_+ e^{i\omega t}$ and $U = e^{iHot/\hbar}$.
The V_I is represented as the operator for time evolution in the interaction picture.
$V_I = \begin{pmatrix} 0 & fe^{i\Delta t} \\ fe^{-i\Delta t} & 0 \end{pmatrix}$ where $\Delta = \omega - \omega_o > 0$.
So for the evolution of Ψ in interaction picture we get:

$$i\hbar \frac{\partial}{\partial t} \begin{pmatrix} e^{-i\omega_o t/2} c_g \\ e^{i\omega_o t/2} c_e \end{pmatrix} = \begin{pmatrix} e^{i\Delta t} f c_e \\ e^{-i\Delta t} f c_g \end{pmatrix} \tag{2.3.4}$$

$$\ddot{c_e} + (i\Delta - \frac{\dot{f}}{f})\dot{c_e} + f^2 c_e = 0 \tag{2.3.5}$$

Our Hamiltonian for the two-level system is described by the following equation $f(t) = \hbar\Omega$=constant(square pulse) :

$$H = -\frac{\hbar\omega_o}{2}\sigma_z + \hbar\Omega e^{i\omega t}\sigma_+ + \hbar\Omega^* e^{-i\omega t}\sigma_- \tag{2.3.6}$$

where the spacing between our two-level system is ω_o. The frequency ω is the frequency of the E/M field that interacts with the quantum dot. Finally, the frequency Ω is called Rabi frequency and it is defined as $\Omega = \frac{d \cdot E}{\hbar}$ where d is the dipole moment which is a feature of the system and E is the envelope function of our pulse. Going to the interaction picture we can get rid of the energy spacing term in the Hamiltonian and reconstruct our new Hamiltonian :

$$\tilde{H} = \hbar\Omega e^{i\Delta t}\sigma_+ + \hbar\Omega^* e^{-i\Delta t}\sigma_- \tag{2.3.7}$$

where $\Delta = \omega - \omega_o$.

We defined the Hamiltonian for our system in the interaction picture and we study the dynamics of the two-level system. We observe the well-studied Rabi oscillations between ground and excited state.

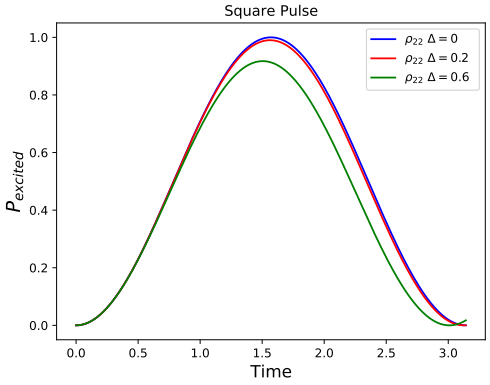

(a) Excited state probability for small detunings of square pulse

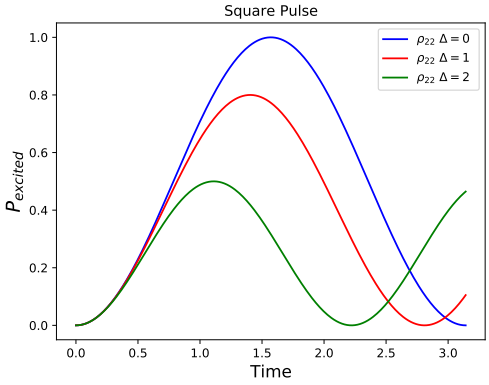

(b) Excited state probability for larger detunings of square pulse

After the famous Rabi oscillations for a square pulse, we can study the trajectory of the spin vector on the Bloch sphere. In the following pictures, we investigate the evolution of spin vector for different detunings.

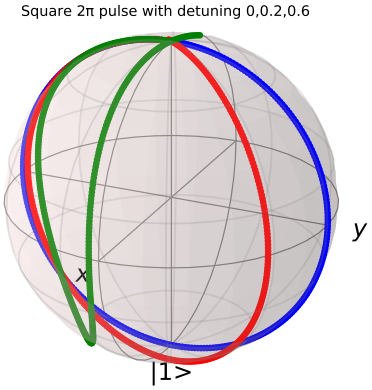

(a) Evolution of spin vector with detuning 0,0.2,0.6 (blue,red,green)

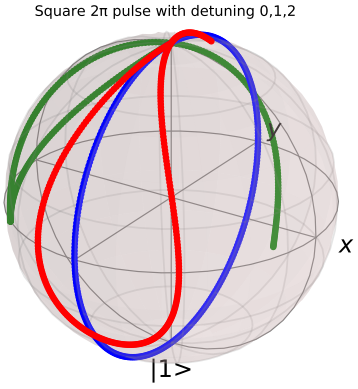

(b) Evolution of spin vector with detuning 0,1,2 (blue,red,green)

The square pulses transfer the population between the excited and the ground state for specific pulses' length. The pulse's duration is directly related to the area of the pulse. Famous areas of pulses are $\pi/2, \pi, 2\pi$. For example, $\pi/2$ pulses rotate the system from the z-axis to the x-axis. The π square pulses rotate the system from the +z to -z-axis and vice versa.

Sech Pulse

There is another famous example of a pulse that is used for manipulating a two-level system. The sech pulse problem is known since the 1930s.[19]

Now we assume that $f(t)$=sech(σt) to specify our problem and after a transformation z=0.5(tanh(σt)+1) we end up with the famous hypergeometrical differential equation.[3] We will investigate the dynamics of the two-level system under the application of a single sech pulse. The following figures are concerning bandwidth σ=1 and the other physical parameters are analyzed with respect to bandwidth.

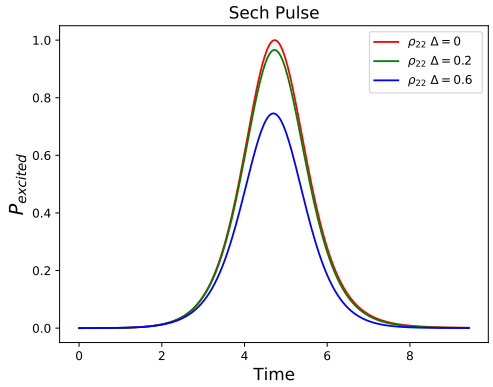

(a) Excited state probability with sech pulse in detuning 0,0.2,0.6

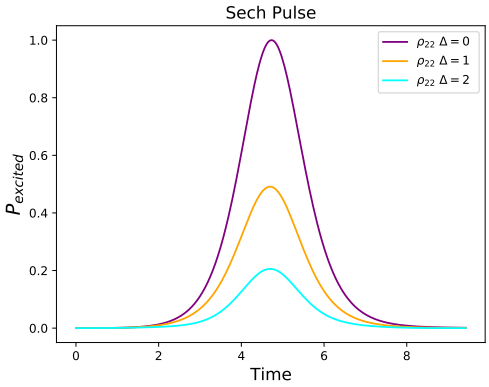

(b) Excited state probability with sech pulse in detuning 0,1,2

The fascinating result is that the sech pulse propagates without losing its shape. So, the detuning affects only the percentage of the transferred population and the period of oscillations is unaffected. We will see how this preserved-shaped pulse affects the coherences in a two-level system.

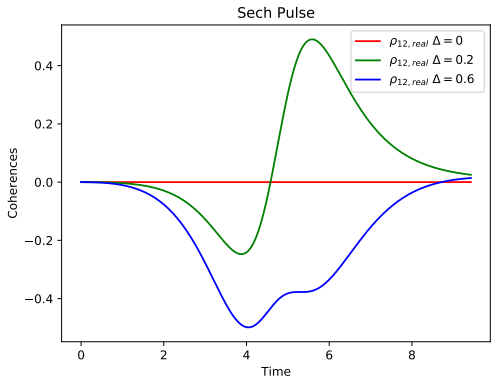

(a) Coherences with Pulse bandwidth $\sigma = 1$ and detunings 0,0.2,0.6

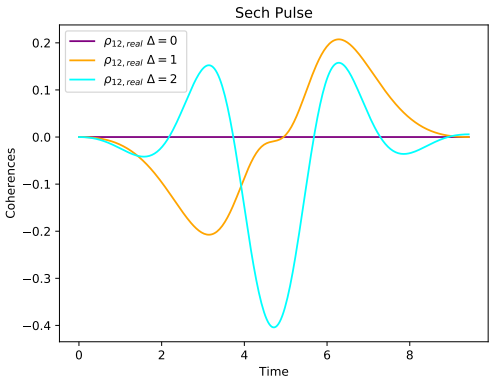

(b) Coherences with Pulse bandwidth $\sigma = 1$ and detunings 0,1,2

For double bandwidth of sech pulse, we have the following coherences in the evolution of time.

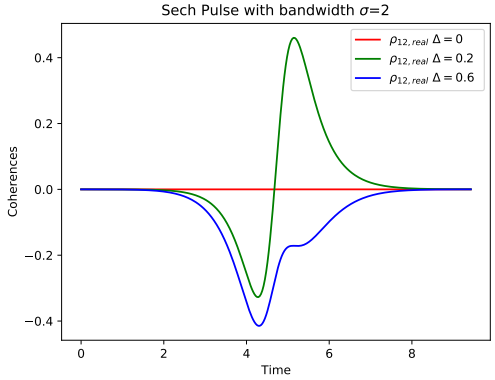

(a) Coherences with pulse bandwidth σ=2 and detunings 0,0.2,0.6

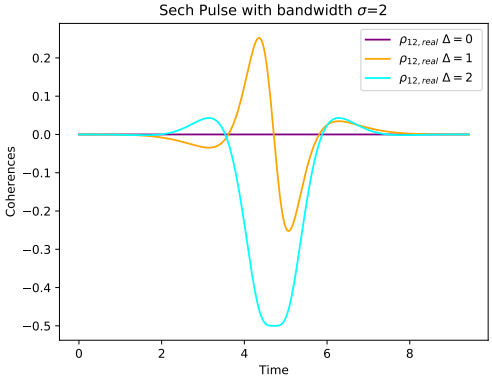

(b) Coherences with pulse bandwidth $\sigma = 2$ and detunings 0,1,2

After the study of density matrix elements, we focus on the Bloch sphere. The following images are about how the state vector of a two-level system evolves under the application of a sech pulse.

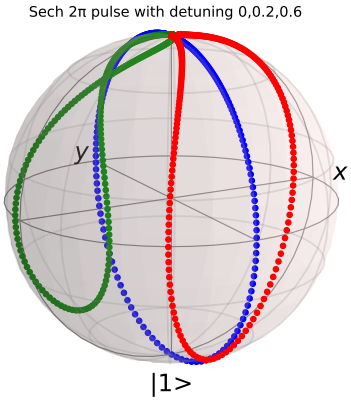

(a) Spin vector dynamics with sech pulse detuned by 0,0.2,0.6 (blue,red,green)

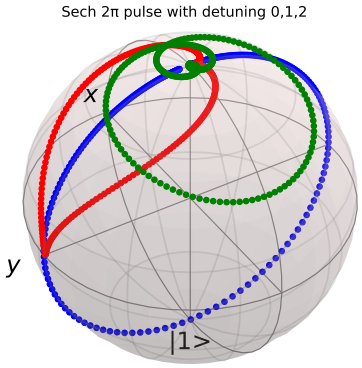

(b) Spin vector dynamics with sech pulse detuned by 0,1,2 (blue,red,green)

2.3.3 Three level system

Going beyond the two-level system, three-level systems are used in QDs to study spin-photon entanglement or optical control.[4] In semiconductor quantum dots the most common example of the three-level Λ system consists of the Zeeman-split states of an excess electron in the QD as ground states and a trion as the excited state. If we apply an in-plane magnetic field we will take advantage of both transitions due to the symmetry breaking.

We can study the dynamics of the three-level system as in the case of the two-level system. We define the Hamiltonian of the three-level system with two E/M laser pulses. In the semiclassical approach, we assume a Λ three-level system.

$$H = \hbar\omega_1 |1\rangle\langle 1| + \hbar\omega_2 |2\rangle\langle 2| + \hbar\omega_3 |3\rangle\langle 3| + \\ \Omega_1 e^{i\omega_a t} |1\rangle\langle 3| + \Omega_1^* e^{-i\omega_a t} |3\rangle\langle 1| + \Omega_2 e^{i\omega_b t} |2\rangle\langle 3| + \Omega_2^* e^{-i\omega_b t} |3\rangle\langle 2|$$

Supposing that the excited state is zero and going in the rotating wave approximation we get:

$$\begin{aligned} \dot{c_1} &= -i\omega_1 c_1 + i\Omega_1(t) e^{i\omega_a t} c_3 \\ \dot{c_2} &= -i\omega_2 c_2 + i\Omega_2(t) e^{i\omega_b t} c_3 \\ \dot{c_3} &= +i\Omega_1^*(t) e^{-i\omega_a t} c_1 + i\Omega_2^*(t) e^{-i\omega_b t} c_2(t) \end{aligned} \tag{2.3.8}$$

In the rotating frame:

$$|\Psi(t)\rangle = \tilde{c_1} |1\rangle + \tilde{c_2} |2\rangle + c_3 |3\rangle \text{ where } \tilde{c_1} = c_1 e^{-i\omega_a t} \text{ and } \tilde{c_2} = c_2 e^{-i\omega_b t} \tag{2.3.9}$$

So the equations (2.3.8) are described as following:

$$\begin{aligned}\dot{\tilde{c_1}} &= -i\Delta_1\tilde{c_1} + i\Omega_1(t)c_3\\ \dot{\tilde{c_2}} &= -i\Delta_2\tilde{c_2} + i\Omega_2(t)c_3\\ \dot{c_3} &= +i\Omega_1^*(t)\tilde{c_1} + i\Omega_2^*(t)\tilde{c_2}\end{aligned}$$

For square pulse:

$$\begin{pmatrix}\dot{\tilde{c_1}}\\ \dot{\tilde{c_2}}\\ \dot{c_3}\end{pmatrix} = -i\begin{pmatrix}\Delta_1 & 0 & -\Omega_1\\ 0 & \Delta_2 & -\Omega_2\\ -\Omega_1^* & -\Omega_2^* & 0\end{pmatrix}\begin{pmatrix}\tilde{c_1}\\ \tilde{c_2}\\ c_3\end{pmatrix}$$

The upper 3×3 matrix is the Hamiltonian of the system. We diagonalize it in order to investigate the dynamics of the three-level Λ system. We assume exact resonance and we solve the eigenvalue problem with the initial condition $c_g(0) = 1$. For eigenvalues:

$$\lambda(-\lambda^2+(|\Omega_1|^2+|\Omega_2|^2)) = 0 \Rightarrow\ \lambda = 0 \text{ or } \lambda = \pm\tilde{\Omega},\ \text{where } \tilde{\Omega} = \sqrt{|\Omega_1|^2+|\Omega_2|^2} \tag{2.3.10}$$

Finding the eigenvectors and going to the dressed state picture we get:

$$c_1(t) = \frac{|\Omega_1|^2}{\tilde{\Omega}^2}\cos\tilde{\Omega}t + \frac{|\Omega_2|^2}{\tilde{\Omega}^2} \tag{2.3.11}$$

$$c_2(t) = -2\frac{\Omega_1^*\Omega_2}{\tilde{\Omega}^2}\sin^2(\frac{\tilde{\Omega}t}{2}) \tag{2.3.12}$$

$$c_3(t) = \frac{i\Omega_1^*}{\tilde{\Omega}}\sin\tilde{\Omega}t \tag{2.3.13}$$

$$\tag{2.3.14}$$

For non resonant square pulses with same detuning($\Delta = \Delta_1 = \Delta_2$) we

get the following answer for the amplitudes of the wavefunction:

$$c_1(t) = e^{-i\Delta t/2}[\frac{i\Delta}{4\sqrt{\tilde{\Omega}^2 + \Delta^2/4}} \sin\left(\sqrt{\tilde{\Omega}^2 + \Delta^2/4}\ t\right) + \frac{|\Omega_1|^2}{\tilde{\Omega}^2} \cos\left(\sqrt{\tilde{\Omega}^2 + \Delta^2/4}\ t\right)]$$

$$+ \frac{e^{i\Delta t}|\Omega_2|^2}{\tilde{\Omega}^2}$$

$$c_2(t) = e^{-i\Delta t/2}[\frac{i\Delta\Omega_2}{4\Omega_1\sqrt{\tilde{\Omega}^2 + \Delta^2/4}} \sin\left(\sqrt{\tilde{\Omega}^2 + \Delta^2/4}\ t\right) + \frac{\Omega_2}{2\Omega_1} \cos\left(\sqrt{\tilde{\Omega}^2 + \Delta^2/4}\ t\right)]$$

$$- \frac{\Omega_2 e^{i\Delta t}}{2\Omega_1}$$

$$c_3(t) = \frac{i|\Omega_1|^2 e^{-i\Delta t/2}}{\Omega_1\sqrt{\tilde{\Omega}^2 + \Delta^2/4}} \sin\left(\sqrt{\tilde{\Omega}^2 + \Delta^2/4}\ t\right)$$

The upper procedure can be used for examining other types of pulses and different detunings in the system.

3 Entanglement in QDs

Entanglement is essential for quantum technologies. There are a couple of ways to generate entanglement in quantum dots. In this chapter, we will study spin-photon entanglement that is crucial for various applications.

3.1 Spin-photon Entanglement

After studying the dynamics of the three-level system driven by a semiclassical field (square pulses), we will get into the quantized E/M field that can explain the entanglement between the spin of the QD and the photons.

The spin-photon entanglement takes advantage of the solid-state system of the QD and its fast recombination rates. Due to the QDs' rates, the qubits recombine and emit single photons to end up with an entangled state. To understand this type of single-photon source, we will investigate the photon degree of freedom with the quantization of the electromagnetic field.

3.1.1 Entanglement protocol

The entanglement between spin and photons starts with an electron in the conduction band.
1) After the in-plane application of the magnetic field, the symmetry breaks.
2) A fast π pulse is applied to transfer the population from ground states to excited states, trion state.
3) Finally, due to the fast recombination rate, the trion state relaxes to the electron states with an emitted photon. We know that this operation produces a highly entangled state between the spin and photon degree of freedom.

The Hamiltonian of the problem consists of a three-level system, a pulse, and a quantized electromagnetic field.

$$H = H_{QD} + H_{pulse-QD} + H_{quantizedE/M+coupling} \tag{3.1.1}$$

The protocol starts with the vacuum field and the equal superposition of ground states. Then the pulse hamiltonian takes place. Finally, the photon due to relaxation entangles with the spin of the QD with a CZ gate. The initial state for our system is $\Psi_{initial} = \frac{1}{\sqrt{2}}(|1\rangle + |2\rangle) \otimes |0_v\rangle$ where $|0_v\rangle$ is the vacuum quantized E/M field. After the application of the pulse the state is $\Psi_{after} = |3\rangle \otimes |0_v\rangle$. Finally, the system relaxes to the ground states emitting a

photon with horizontal and vertical polarization. So the final state is defined as :

$$\Psi = \frac{1}{\sqrt{2}}(|1\rangle \otimes |H\rangle + |2\rangle \otimes |V\rangle) \tag{3.1.2}$$

where $|H\rangle = a_H^\dagger |0_v\rangle, |V\rangle = a_V^\dagger |0_v\rangle$. The operator $a_{H,V}^\dagger$ is the creation of photon in the horizontal and vertical mode respectively. The upper state is entangled as long as there is no way to be written in a separable form.

So it is clear that it produced an entangled state between spin and photon. To identify how good is the entanglement we measure the fidelity of the entangled gate between spin and photon.

3.1.2 Results

The spin degree of freedom becomes entangled with the photon's polarization in a GHZ state(1.3.4). GHZ state is the local equivalent to a two-qubit cluster state. We assume that our photon is stored in a cavity or a fiber that has coupling g $\approx \mu eV$.

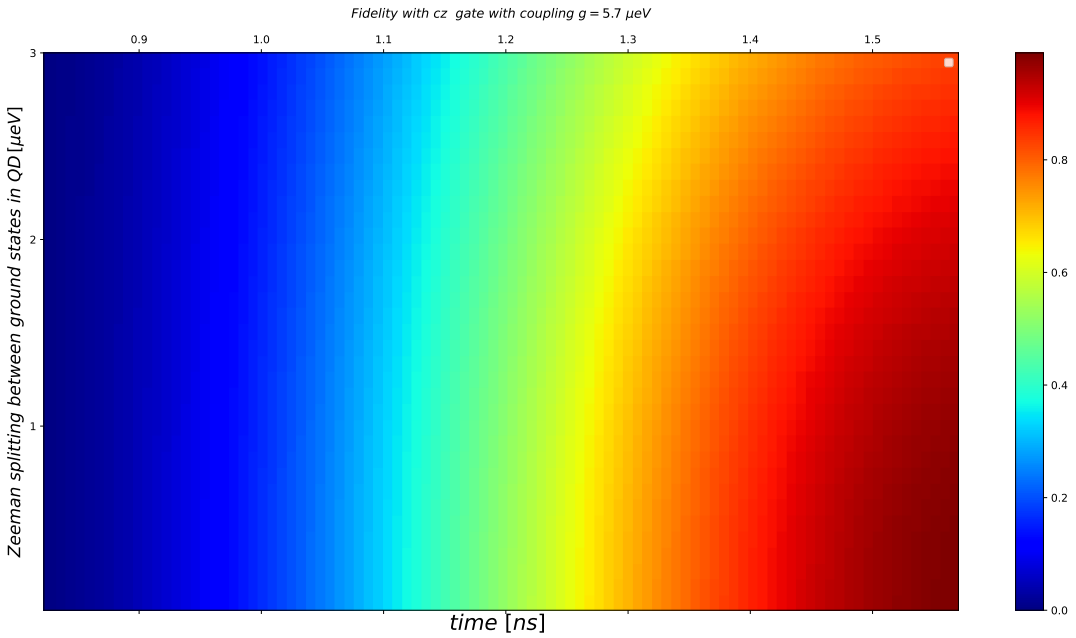

Figure 19: Fidelity of CZ gate with spin-photons

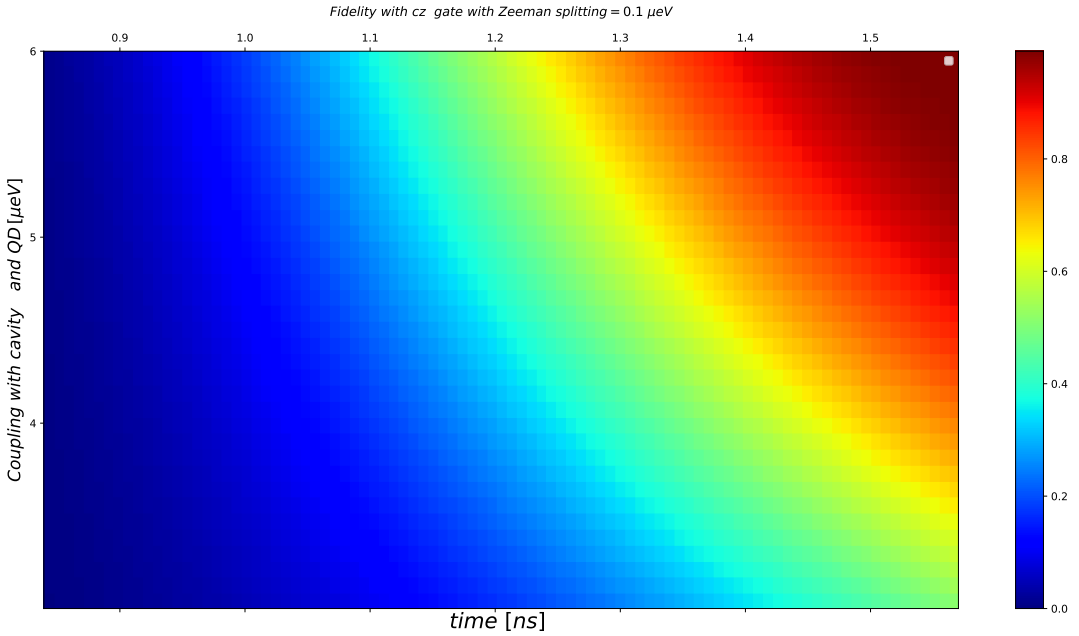

Figure 20: Fidelity of CZ gate with spin-photons

3.2 Multipartite Entanglement using QDs

Multiphoton entanglement is generated with a photonic machine gun.[12, 20] The protocol consists of a periodical pumping of the population in ground states to excited states through a pulse train. The repeated pumping will generate one photon in each cycle with specific polarization modes that are entangled with the spin degree of freedom. In this way, we can continue the process to end up with lots of entangled photons entangled with the spin. This protocol can produce the famous GHZ state of photons.(1.3.4)

Multi-QDs entanglement

Instead of using photons for entanglement, there is a possibility of producing the well-known spin-spin entanglement between coupled quantum dots. This type of entanglement is well studied in the quantum electronics regime with gated quantum dots.[21, 22, 23] The use of spin-spin entanglement with coupled dots and spin-photon entanglement with periodical pumping can generate 2d cluster states which are capable of universal quan-

tum computing.[12, 24]

4 Entanglement Purification

After the generation of photonic cluster states with semiconductor self-assembled quantum dots, we can use them for quantum computation.

However, the entanglement that is generated in experiments is weak. For instance, to generate a cluster state we perform CZ gates between the qubits. Although in experiments, the generation of the cluster state may be imprecise. Instead of the application of the CZ gate, Cphase(1.3.3) gates appear. These gates will not generate a cluster state but a state with weaker entanglement between nodes due to the Cphase gate. So we have to purify the state to obtain the highly entangled state.

The two-qubit gates which perform the entanglement must be close to the ideal case. There are different ways to make highly entangled states. Lots of quantum error-correcting codes exist that consume redundant qubits to create states of fewer qubits that are closer to perfect entangled states.[25, 26]

On the other hand, there is entanglement purification[27] that uses LOCC and produces higher entangled states using weaker entangled states. The simplest example is purifying a bipartite system. To produce a Bell state, we make LOCC in weak two-qubit entangled states. In the following section, we will see how it is possible to generate them.

4.1 Bipartite system

4.1.1 Bennett et al. protocol

In 1995, Bennett et al.[28] proposed a way to distill a two-qubit entangled state from two weak entangled states. The steps of the protocol are the following:
1)Generate two partially entangled states between Alice and Bob.
2)Make local operations and transfer each state to Werner state.(4.1.2)
3)Make bilateral CNOT(1.3.2) operators in Alice's qubits and Bob's qubits respectively.
4)Measure one qubit of Alice and Bob.

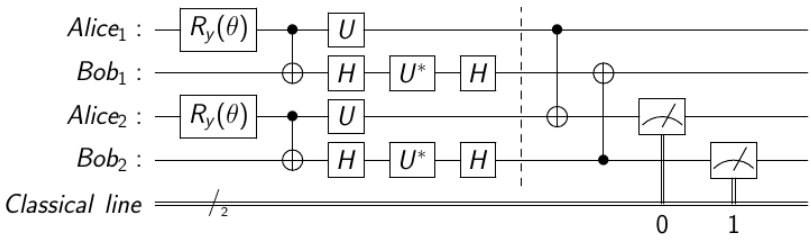

Figure 21: Bennett et al. protocol

If the measurements coincide (00 or 11) then we can iterate the protocol. The iterations will increase our fidelity with the entangled state of the unmeasured qubits. If the measurements are different the unmeasured state is discarded.

After the creation of the partially entangled states, the following step is to produce a Werner state. We start by producing the bipartite system in the diagonal Bell basis by applying the stabilizer operators of Bell states probabilistically. After applying the stabilizer operators, we get the desired diagonal density matrix in Bell basis.

$$\rho_{bell} = p_0 \left|\Psi^+\right\rangle \left\langle\Psi^+\right| + p_1 \left|\Psi^-\right\rangle \left\langle\Psi^-\right| + p_2 \left|\Phi^+\right\rangle \left\langle\Phi^+\right| + p_3 \left|\Phi^-\right\rangle \left\langle\Phi^-\right| \quad (4.1.1)$$

where p_i are real numbers that satisfy the relation $\sum_{i=0}^{3} p_i = 1$.

To further depolarize the state we apply random unitary gates and Hadamard gates in a specific way to get to a Werner state. Mathematically speaking a Werner state is :

$$\rho_{werner} = p_0 \left|\Psi\right\rangle \left\langle\Psi\right| + p_1 I_{AB} \quad (4.1.2)$$

where $|\Psi\rangle$ is one of the Bell states $(\Psi^{+,-}, \Phi^{+,-})$ and I_{AB} is the 4x4 identity matrix for the bipartite system.

Specifically for creating a Werner state the first step is to apply a random unitary matrix U to Alice's qubits. After that, we apply a Hadamard gate, the conjugate of the random unitary matrix which was first applied and finally the Hadamard gate again in Bob's qubits. The procedure can be seen in the picture above. In that way, we have the desired Werner state of each entangled state.[27]

The next step was to apply the local CNOT gates.
We perform CNOT gates for qubits of each observer (Alice and Bob). This step is crucial because it transforms the information from Ψ states to Φ states and the fidelity is getting higher.

Finally, Bob measures one qubit and Alice another one. If the measurements are the same, the state of the unmeasured qubits is kept, otherwise is discarded.

4.1.2 Deutsch et al. protocol

Deutsch et al. in 1996[29] proposed a protocol that can create Bell states without applying random unitary gates and stabilizer operators.

Instead of producing a Werner state as in the Bennett et al. protocol, we apply specific operations to Alice's and Bob's qubits. We perform an $R_x(\pi/2)$ rotation for Alice qubits and its adjoint $R_x(-\pi/2)$ rotation to Bob qubits instead of transforming our entangled state into Werner state. The other steps are identical to the Bennett et al. protocol.[28]

It is pretty straightforward to see how our state is changed through this protocol. We begin with two partially entangled states

$$|\Psi_1\rangle\,|\Psi_2\rangle = (a\,|0_A0_B\rangle + b\,|1_A1_B\rangle)\;(c\,|0_A0_B\rangle + d\,|1_A1_B\rangle). \tag{4.1.3}$$

To simplify the calculations we assume that $a = c$ and $b = d$ which means that we begin with two identical entangled states. We perform the operation $R_x(\pi/2)$ for Alice's qubits and the adjoint one for Bob's qubits.

$$|0_A\rangle \to \frac{|0_A\rangle - i\,|1_A\rangle}{\sqrt{2}} \;\; |1_A\rangle \to \frac{|1_A\rangle - i\,|0_A\rangle}{\sqrt{2}}$$
$$|0_B\rangle \to \frac{|0_B\rangle + i\,|1_B\rangle}{\sqrt{2}} \;\; |1_B\rangle \to \frac{|1_B\rangle + i\,|0_B\rangle}{\sqrt{2}}$$

After performing this step we can apply the CNOT gates for Alice's and Bob's qubits. About Bob's qubits, we apply the CNOT gate with control and target qubits with swapping roles.

$$|00_A\rangle \to |00_A\rangle\,,\;\; |00_B\rangle \to |00_B\rangle$$
$$|01_A\rangle \to |01_A\rangle\,,\;\; |01_B\rangle \to |11_B\rangle$$
$$|10_A\rangle \to |11_A\rangle\,,\;\; |10_B\rangle \to |10_B\rangle$$
$$|11_A\rangle \to |00_A\rangle\,,\;\; |11_B\rangle \to |01_B\rangle$$

We take the adjoint of the state to get the full matrix of the two entangled states. After that, we trace out to take the information for the unmeasured

subsystem.

$$\rho = \frac{(a+b)^4}{4}\left|\Phi^+\right\rangle\left\langle\Phi^+\right| + \frac{(a^2-b^2)^2}{4}\left|\Psi^-\right\rangle\left\langle\Psi^-\right| + \frac{(a^2-b^2)^2}{4}\left|\Phi^-\right\rangle\left\langle\Phi^-\right| + \frac{(a-b)^4}{4}\left|\Psi^+\right\rangle\left\langle\Psi^+\right|$$

Taking advantage of the upper equation we can compute our new fidelity. After some iterations, the state of the unmeasured qubits reaches the Bell state. We will study the reachable fidelity and how the initial fidelity is increased after each iteration.

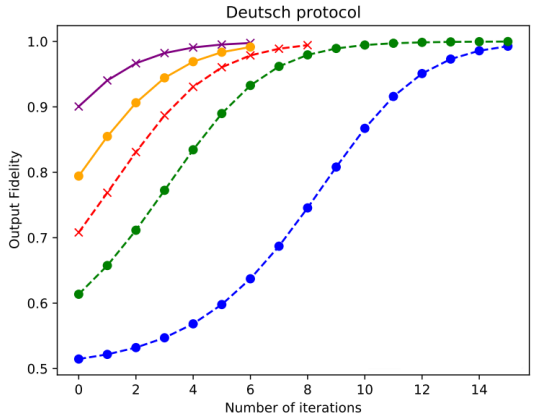

(a) Purification of a two-qubit entangled state using two identical partially entangled states of initial fidelity 0.5, 0.6, 0.7, 0.8, 0.9 (blue, green, red, yellow, purple line) .

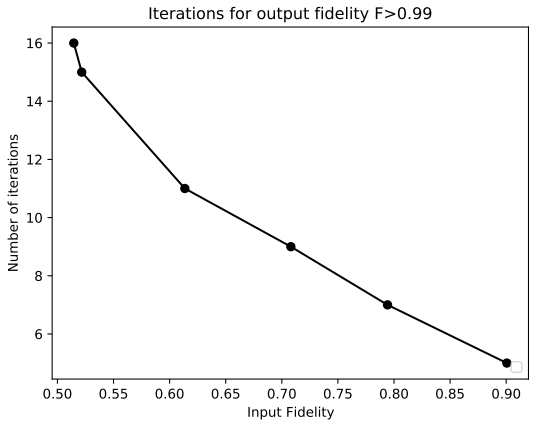

(b) Iterations of protocol to reach fidelity F=0.99.

Figure 22: Final fidelity with Deutsch et al. protocol.

Bipartite purification with noisy operations

After studying the whole protocol, we can see the crucial usage of one and two-qubit operations to purify one entangled state. In experiments, there are errors between qubit gates. In the following figures, we will assume that each qubit gate can be a depolarizing channel of probability p.

The depolarizing channel for each qubit gate is defined as :

$$E(\rho) = (1-p)\rho + p\frac{I}{2}$$

We use the Deutsch et al. protocol with single error gates and we get the maximum fidelity that can be reached.

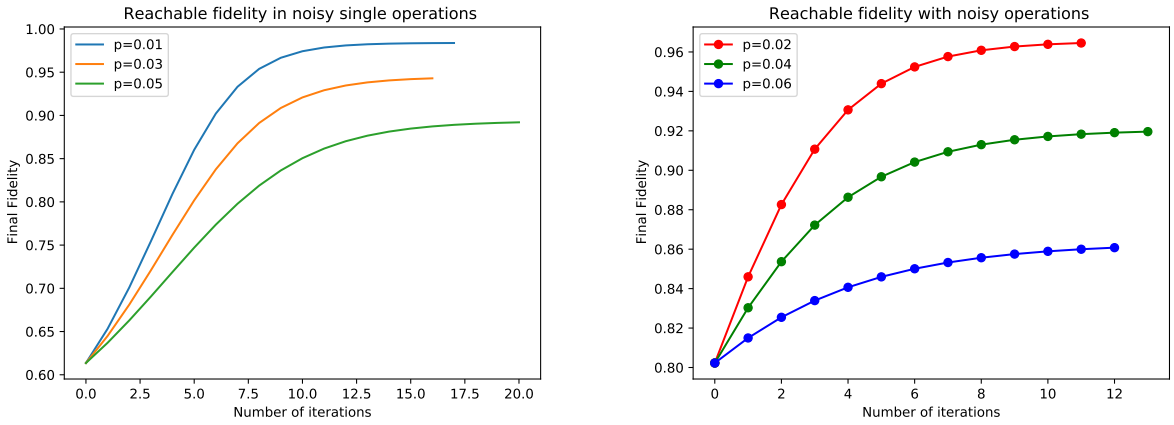

Figure 23: Fidelity of state after purification with noisy operations.

4.1.3 Comparison between Deutsch et al. and Bennett et al. protocols

The Deutsch et al. protocol is efficient. There is no need to go to the Werner state through applications of random unitary gates. The output fidelity in Bennett et al. protocol is well established.[27]

$$F' = \frac{F^2 + (1-F)^2/9}{F^2 + 2F(1-F)/3 + 5(1-F)^2/9} \tag{4.1.4}$$

We found the output fidelity in Deutsch et al. protocol and we compare it with the Bennett et al. protocol.

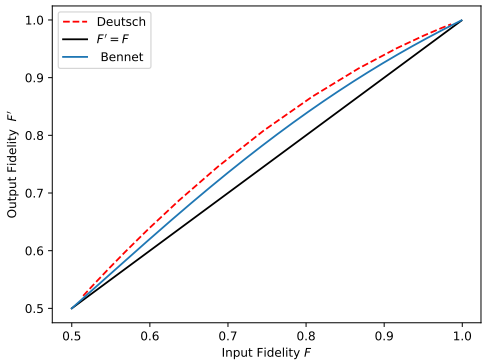

Figure 24: Output fidelity after iterating the protocol once with initial fidelity.

The output fidelity in the Deutsch et al. protocol is higher than the Bennett et al. protocol. So, the specific operations in the Deutsch et al. protocol are more efficient for the asymptotically perfect fidelity.

4.2 Multipartite system

In multipartite systems, the process of entanglement purification is a little bit trickier. There is no way to apply specific operations like in the Deutsch et al. protocol, so we adapt the Bennett et al. protocol for multipartite systems. [27, 30, 31, 32, 33]

The protocol is an extended version of Bennett et al. protocol with multipartite entangled states. Steps for the purification of multi-qubit entangled states:
1)Create two weak multi-qubit entangled states with the same fidelity.
2)Apply probabilistic stabilizer operators in each entangled state.
3)Apply the local CNOTs between qubits of the same group.
4)Measure the qubit of the one weak multi-qubit entangled state.

If $\sum_i^N M_i \oplus 2 = 0$, where the outcomes of the measurement operators are M_i, we keep the unmeasured state, otherwise we discard it. Now we will present the quantum circuits and the improved fidelities for famous multi-qubit entangled states. The expansion to entangled states with more qubits is pretty straightforward.

4.2.1 Purification with identical copies

The traditional protocol for purifying a graph state uses two identical copies of the graph.

Suppose we begin with two partially entangled graph states. We apply the stabilizer operators of the state in a probabilistic way and we end up with a state that is diagonal on a graph state basis. After the application of stabilizers, we perform the CNOT gates between qubits of the same group. For qubits that belong on another group of vertices, we apply CNOT gates swapped, assuming that the control qubit belongs to the second state and the target in the first one.

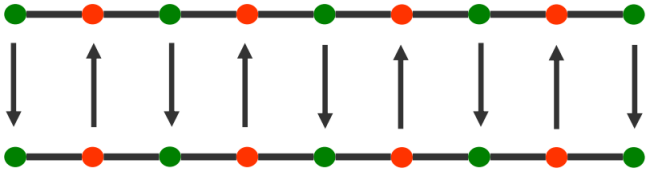

Figure 25: Schematic for the applied CNOT gates in a graph state[27].

Specific examples of purification of multipartite systems can be seen in the following figures.

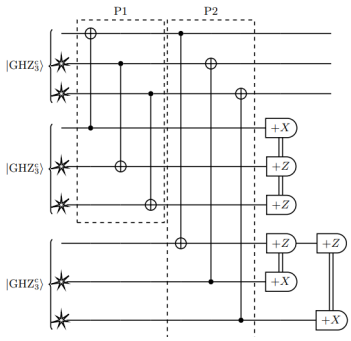

(a) Quantum circuit for purifying GHZ states[31]

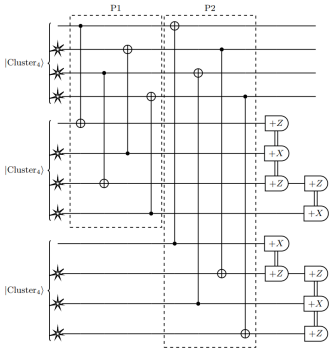

(b) Quantum circuit for purifying cluster states[31]

The stars in the upper figures denote the partially entangled states and the measurements are on an X and Z basis. The protocol is a probabilistic application of P_1 and P_2 subprotocols. The P_1 purifies the entanglement for the first qubit in the weak entangled state and the P_2 purifies the entanglement connection between the other qubits. Now we will use this type of quantum circuit. We will produce the post-distillation for the GHZ states consuming a weak GHZ state after every iteration.

Except for the creation of GHZ state, cluster state purification is important for measurement-based quantum computation. The protocol is identical to the GHZ state.

After the GHZ and the cluster state protocol, we can apply these operations to another graph state as long as the initial entangled states are the same. The measurements on the qubits of the first graph will purify and increase the entanglement between the qubits of the second one. The errors in multipartite systems are more common than in bipartite systems. Noisy operations are more likely to be present in multi-qubit states than in the bipartite state.

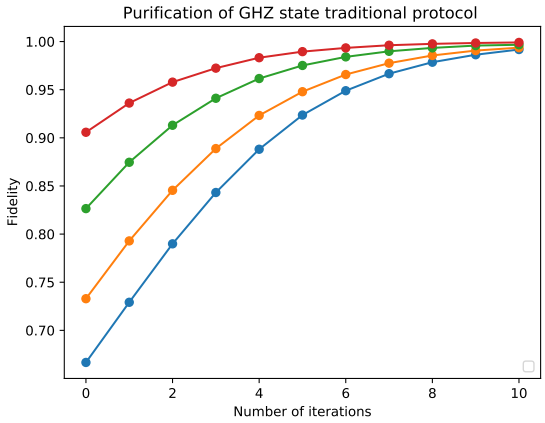

(a) Purification protocol using two partially entangled states with initial fidelities 0.65, 0.72, 0.82, 0.9 (blue, orange, green, red line) to reach a three-qubit GHZ state(1.3.4)

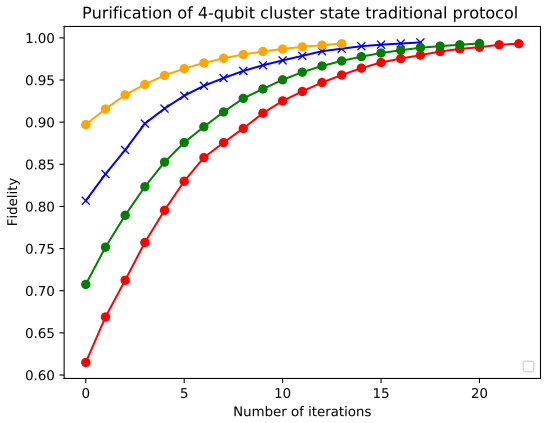

(b) Purification protocol using two partially entangled states with initial fidelities 0.61, 0.71, 0.81, 0.89 (red, green, blue, yellow line) to reach a four-qubit cluster state

4.3 Purification of two-qubit states after measurements

The following work is original and produces new knowledge about the purification of two-qubit states using measurements. We start with a partially entangled multi-qubit state that is close to a linear cluster state and we perform measurements in the middle qubits to get a highly entangled state of the end qubits.

Highly entangled states are difficult to create. In experiments, there is a high probability of creating Cphase gates instead of the CZ gates. A single QD can generate a Cphase gate with photons[34, 35]. Time-bin entangled photons[36] is another example for generating entanglement through Cphase gates. However, Bell states are essential for the creation of the quantum network.[37]

First, we initialize our protocol with a linear state of three or more qubits that are connected via Cphase gates. Graphs created using Cphase gates are called weighted graphs.[6] We perform X basis measurements on the middle qubits and measure the entanglement of the two end qubits that remain unmeasured.

The X basis measurements purify the system of the two end qubits and the final two-qubit state of the unmeasured qubit can become a Bell pair. We will investigate the three, four, and five-qubit cases and see the purification of the unmeasured qubits concerning the θ angle of Cphase gates.

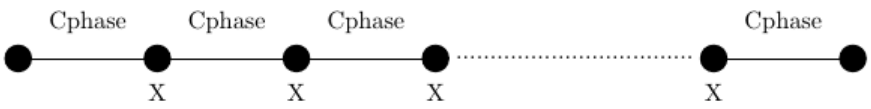

Figure 28: Schematic for the general protocol

After the X measurements we purify the state of the first and the last qubit and we measure the concurrence.

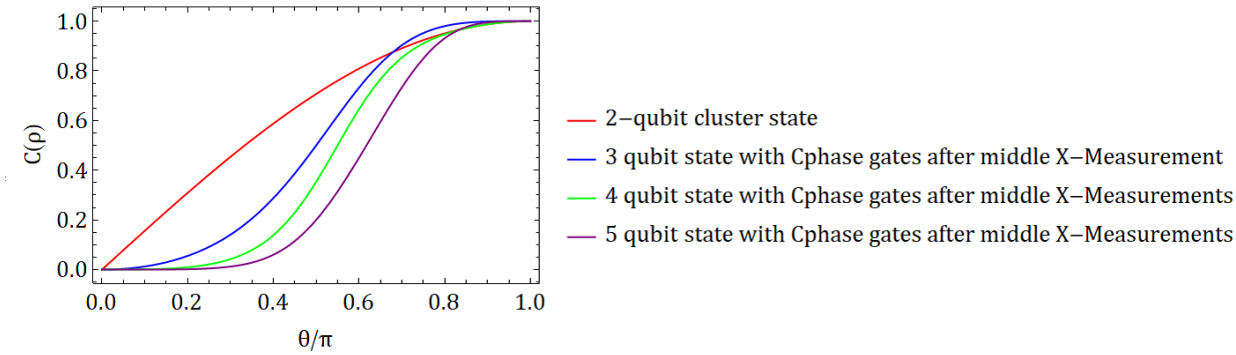

Figure 29: Concurrence of the two end qubits after the X measurements of the middle ones.

It seems that in the case of an even number of qubits in an entangled state if we measure the middle qubits there is no purification. However, in the case of three and five qubits, measuring in the X basis the middle qubits increases the entanglement of the two-qubit state maximizing the concurrence for nonideal entangling gates.

We try the star graph and purify its two qubits after applying X basis measurements to the other ones.

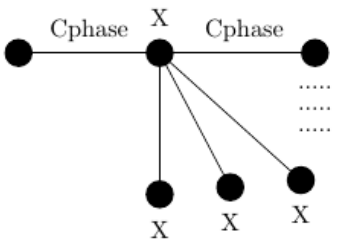

Figure 30: Schematic for the star graph.

In the star graph with Cphase gates between qubits, there is no purification as the system grows. The purification takes place for a specific part of the angle in the Cphase gates.

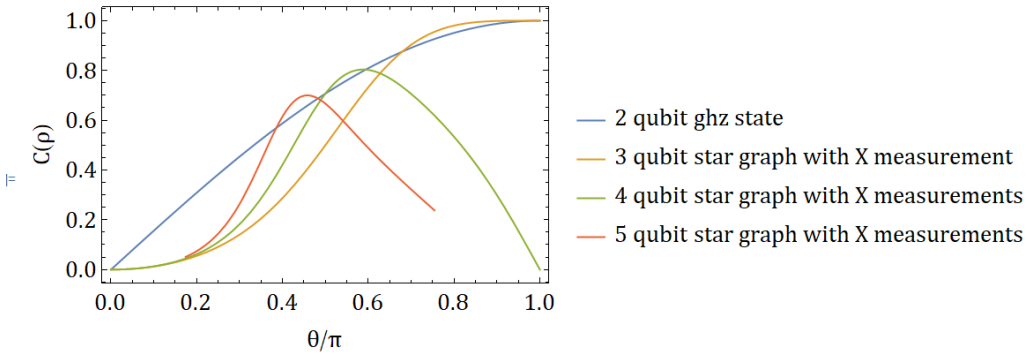

Figure 31: Concurrence of the two qubits after X measurements of the other ones in the star graph.

Understanding how to extract smaller multipartite states of higher entanglement out of larger weighted graphs is a topic of fundamental and practical interest, which we are investigating in ongoing work.

5 Conclusions

Self-assembled semiconductor quantum dots are single-photon sources and promising candidates for the generation of photonic entanglement. They can create photons that can become entangled with the spin qubits of the QD. These entangled states can be made deterministically by using pulses and a fiber to store the photons. By performing a periodic train of pulses to manipulate the spin qubit in the QD, we can emit photons that can become entangled with the spin of the QD.

However, there is a possibility of creating a partially entangled state if the operations (pulses) are induced to errors and are imperfect. In this case, we can use an approach of quantum information science to increase the entanglement. The application of local operations and two-way quantum communication is enough to purify our entangled state. Photonic entangled states and the idea of entanglement purification are well-known in quantum networks with the use of quantum repeaters.[38, 39, 40]

References

[1] DiVincenzo, David P.,*The Physical Implementation of Quantum Computation*, Fortschritte der Physik. 48 (9–11): 771–783.

[2] Michael A. Nielsen, and Isaac L. Chuang, *Quantum Computation and Quantum Information*, Cambridge University Press

[3] Sophia E. Economou, L. J. Sham, Yanwen Wu, and D. G. Steel, *Proposal for optical U(1) rotations of electron spin trapped in a quantum dot*, Phys. Rev. B 74, 205415

[4] Ren-Bao Liu, Wang Yao, and L. J. Sham, *Quantum computing by optical control of electron spins* ,arXiv:1006.5544v1 2010

[5] `https://en.wikipedia.org/wiki/Spontaneous_parametric_down-conversion`

[6] M. Hein, W. Dür, J. Eisert, R. Raussendorf, M. Van den Nest,and H H.-J.Briegel, *Entanglement in Graph States and its Applications*, https://arxiv.org/abs/quant-ph/0602096

[7] Geza Toth, and Otfried Guehne, *Entanglement Detection in the Stabilizer Formalism* , arXiv:quant-ph/0501020v2 2005

[8] Daniel A. Marcus, *Graph Theory: A Problem Oriented Approach* MAA Textbooks 2008

[9] Robin J. Wilson, *Introduction to Graph Theory* Pearson 2010

[10] Olaf Mandel, Markus Greiner, Artur Widera, Tim Rom, Theodor W. Hänsch and Immanuel Bloch, *Controlled collisions for multiparticle entanglement of optically trapped atoms*, Nature volume 425, pages937–940(2003)

[11] PhD thesis: Oliver William Seton Tedder, *Monitoring the spin environment of coupled quantum dots: towards the deterministic generation of photonic cluster states*,University College London 2018

[12] Mercedes Gimeno-Segovia, Terry Rudolph, and Sophia E. Economou, *Deterministic Generation of Large-Scale Entangled Photonic Cluster State from Interacting Solid State Emitters*, Phys. Rev. Lett. 123, 070501 2019

[13] Robert Raussendorf and Hans J. Briegel, *A One-Way Quantum Computer* , Phys. Rev. Lett. 86, 5188 2001

[14] Pascale Senellart, Glenn Solomon and Andrew White, *High-performance semiconductor quantum-dot single-photon sources*, Nature Nanotechnology volume 12, pages1026–1039(2017)

[15] Wang, Zhiming M *Self-Assembled Quantum Dots* , Springer 2008

[16] I. Saidi, S. Ben Radhia, and K. Boujdaria, *Band parameters of GaAs, InAs, InP, and InSb in the 40-band kp model*, Journal of Applied Physics 107, 043701 (2010)

[17] Payal Bhardwaj*, Nupur Das, *Exciton binding energy in bulk and quantu well of semiconductors with non-parabolic energy bands*,IJESRT 10.5281/zenodo.166850 2016

[18] S. Gustavsson, R. Leturcq, T. Ihn, K. Ensslin and A. C. Gossard, *Electrons in quantum dots: One by one*, Journal of Applied Physics 105, 122401 (2009)

[19] N. Rosen and C. Zener, *Double Stern-Gerlach Experiment and Related Collision Phenomena*,Phys. Rev. 40, 502 – 1932

[20] Netanel H. Lindner and Terry Rudolph, *Proposal for Pulsed On-Demand Sources of Photonic Cluster State Strings*,Phys. Rev. Lett. 103, 113602 2009

[21] John Schliemann and Daniel Loss, *Entanglement and Quantum Gate Operations with Spin-Qubits in Quantum Dots*, arXiv:cond-mat/0110150v1 2001

[22] Tetsufumi Tanamoto, Shigeji Fujita, X. Hu and Y.-X. Liu, *Cluster states in charge qubits based on coupled quantum dots*, AIP Conference Proceedings 893, 1105 (2007)

[23] Sinan Bugu, Fatih Ozaydin, Thierry Ferrus and Tetsuo Kodera, *Preparing Multipartite Entangled Spin Qubits via Pauli Spin Blockade*,Scientific Reports volume 10, Article number: 3481 (2020)

[24] M Van den Nest, W Dür, A Miyake and H J Briegel, *Fundamentals of universality in one-way quantum computation* ,New J. Phys. 9 204 2007

[25] Daniel Gottesman, *An Introduction to Quantum Error Correction and Fault-Tolerant Quantum Computation*, arXiv:0904.2557v1 2009

[26] Barbara M. Terhal, *Quantum Error Correction for Quantum Memories*, arXiv:1302.3428v7 2013

[27] W. Dür, and H. J. Briegel, *Entanglement purification and quantum error correction*, arXiv:0705.4165v2 2007

[28] Charles H. Bennett, Gilles Brassard, Sandu Popescu, Benjamin Schumacher, John A. Smolin,and William K. Wootters, *Purification of Noisy Entanglement and Faithful Teleportation via Noisy Channels* , arXiv:quant-ph/9511027v2 1995

[29] David Deutsch, Artur Ekert, Richard Jozsa, Chiara Macchiavello, Sandu Popescu, and Anna Sanpera, *Quantum Privacy Amplification and the Security of Quantum Cryptography over Noisy Channels*,Phys. Rev. Lett. 77, 2818 1996

[30] H. Aschauer, W. Dür, and H.-J. Briegel, *Multiparticle entanglement purification for two-colorable graph states*,arXiv:quant-ph/0405045v2 2004

[31] Stefan Krastanov, Alexander Sanchez de la Cerda, and Prineha Narang, *Heterogeneous Multipartite Entanglement Purification for Size-Constrained Quantum Devices*, arXiv:2011.11640v1 2020

[32] W Dür , H Aschauer, H-J Briegel, *Multiparticle entanglement purification for graph states*,PhysRevLett.91.107903 2003

[33] Caroline Kruszynska, Akimasa Miyake, Hans J. Briegel, and Wolfgang D¨ur, *Entanglement purification protocols for all graph states*,arXiv:quant-ph/0606090v2 2006

[34] Hyochul Kim, Ranojoy Bose, Thomas C. Shen, Glenn S. Solomon and Edo Waks, *A quantum logic gate between a solid-state quantum bit and a photon*, Nature Photonics volume 7, pages373–377(2013)

[35] Yu Shi and Edo Waks, *Deterministic generation of multi-dimensional photonic cluster states using time-delay feedback*, arXiv:2101.07772v1

[36] Hsin-Pin Lo, Takuya Ikuta, Nobuyuki Matsuda, Toshimori Honjo and Hiroki Takesue, *Entanglement generation using a controlled-phase gate for time-bin qubits*, Appl. Phys. Express 11 092801 (2018)

[37] Wojciech Kozlowski and Stephanie Wehner, *Towards Large-Scale Quantum Networks*, arXiv:1909.08396v1

[38] W Dür,H.- J. Briegel,J. I. Cirac and P. Zoller, *Quantum repeaters based on entanglement purification*, Phys.Rev.A59:169,1999

[39] Nicolas Sangouard, Christoph Simon, Hugues de Riedmatten and Nicolas Gisin, *Quantum repeaters based on atomic ensembles and linear optics*, arXiv:0906.2699v2 2009

[40] Koji Azuma, Kiyoshi Tamaki and Hoi-Kwong Lo, *All-photonic quantum repeaters*, Nature Communications volume 6, Article number: 6787 (2015)

[41] J. R. Johansson, P. D. Nation, and F. Nori, *QuTiP: An open-source Python framework for the dynamics of open quantum systems.*, Comp. Phys. Comm. 183, 1760–1772 (2012) [DOI: 10.1016/j.cpc.2012.02.021].

[42] G. Aleksandrowicz et al., *Qiskit: An open-source framework for quantum computing*, 2019